Photonic band gap filter for wavelength division multiplexer

A. D'Orazio, M. De Sario, V. Petruzzelli, F. Prudenzano

Dipartimento di Elettrotecnica ed Elettronica – Politecnico di Bari, Via Re David, 200 –70125 Bari -Italy
dorazio@poliba.it, petruzzelli@poliba.it

Abstract: An optical multiplexer-demultiplexer based on an index-confined photonic band gap waveguide is proposed. The dropping of electromagnetic waves having a given frequency or a certain frequency band is obtained via a phase-shifted grating obtained by breaking the uniform period sequence to include a defect layer. The selective filtering properties of the proposed structure are simulated by means of a computer code relying on a bi-directional beam propagation method based on the method of lines.

OCIS codes: (060.4230) Multiplexing; (230.7370) Waveguides

References and Links

1. J.D. Joannopoulos, R.D. Meade, and J.N. Winn, *Photonic Crystals. Molding the Flow of Light*", (Princeton University Press, 1995).
2. A.D'Orazio, M.De Sario, V.Petruzzelli, F.Prudenzano: "Numerical modeling of photonic band gap waveguiding structures", Recent Research Developments in Optics, S.G.Pandalai Editor, 2002.
3. S. Fan, P. R. Villeneuve, J. D. Joannopoulos, and H. A. Haus, "Channel drop tunneling through localized states," Phys. Rev. Lett. **80**, 960–963 (1998).
4. C. Jin, S. Han, X. Meng, B. Cheng, and D.Zhang, "Demultiplexer using directly resonant tunneling between point defects and waveguides in a photonic crystal," J. Appl. Phys. **91**, 4771–4773 (2002).
5. H.Kosaka,T.Kawashima, A.Tomita, M.Notomi, T.Tamamura, T.Sato and S.Kawakami, "Photonic crystals for micro lightwave circuits using wavelength-dependent angular beam steering," Appl. Phys. Lett. **74**, 1370-1372 (1999).
6. S. Noda, A. Chutinan, and M. Imada, "Trapping and emission of photons by a single defect in a photonic bandgap structure," Nature, **407**, 608–610 (2000).
7. B. E. Nelson, M. Gerken, D. A. B. Miller, R. Piestun, C.-C. Lin, and J. S. Harris, "Use of a dielectric stack as a one-dimensional photonic crystal for wavelength demultiplexing by beam shifting," Opt. Lett. **25**, 1502–1504 (2000).
8. M. Koshiba, "Wavelength division multiplexing and demultiplexing with photonic crystal waveguide couplers," J. Lightwave Technol. **19**, 1970–1975 (2001).
9. A. Sharkawy, S. Shi, and D. W. Prather, "Multichannel wavelength division multiplexing with photonic crystals," Appl. Opt. **40**, 2247–2252 (2001).
10. E. Ozbay, M. Bayindir, I. Bulu, and E. Cubukcu, "Investigation of localized coupled-cavity modes in two-dimensional photonic band gap structures," IEEE J. Quantum Electron. **38**, 837–843 (2002).
11. S.Y.Lin, J.G.Fleming, "A three-dimensional Optical Photonic Crystal," J.Lightwave Technol., **17**, 1944-1947, (1999).
12. R.Kashyap, *Fiber Bragg Gratings*, (Academic press, San Diego, 1999).
13. G.I.Stegeman, D.G.Hall, "Modulated index structure," J.Opt. Soc. Am. A, **7**, 1387-1398 (1996).
14. C.R.Giles, "Lightwave applications of fiber Bragg gratings," J.Lightwave Technol., **15**, 1391-1404, (1997).
15. R.W.Ziolkowski, T.Liang, "Design and characterization of a grating-assisted coupler enhanced by a photonic-band-gap structure for effective wavelength-division demultiplexing," Optics Letters, **22**, 1033-1035, (1997).
16. C.F.Lam, R.B.Vrijen, P.P.L.Chang-Chien, D.F.Sievenpiper, E.Yablonovitch, "A tunable wavelength demultiplexer using logarithmic filter chains," J. Lightwave Technol. **16**, 9, 1657-1662, (1998).
17. R.Zengerle, O.Leminger, "Phase shifted Bragg-grating filters with improved transmission characteristics," J. Lightwave Technol., **13**, 2354-2358, (1995).
18. L.Wei, J.W.Y.Lit, "Phase-shifted Bragg Grating Filters with symmetrical structures," J. Lightwave Technol., **15**,1405-1410, (1997).
19. A. D'Orazio, M. De Sario, V. Petruzzelli, F. Prudenzano: "Bidirectional Beam Propagation Method based on the Method of Lines for the Analysis of Photonic Band Gap Structures," accepted for publication in Optical and Quantum Electronics, 2002.
20. S.Helfert, R.Pregla, "Efficient analysis of periodic structures," J. Lightwave Technol., **16**, 1694-1702, (1998).

#1976 - $15.00 US Received December 19, 2002; Revised February 03, 2003

21. G. Murtuza, J. M. Senior, "Analytical tools for the assessment of optical crosstalk in WDM systems," IEE Colloquium on, Digest **1997/036**, 16/1-16/4, (1997).

1. Introduction

The evolution of optical networks has progressed from single wavelength point-to point data links, to multiple wavelength fixed data links, and to fully reconfigurable multiple wavelength systems. Commercially available network elements such as add-drop multiplexers, optical crossconnects and wavelength amplifiers can be used to build flexible network architectures which can carry terabits of information and handle the interconnection of internet protocol routers, asynchronous transfer mode (ATM) switches, and synchronous optical network (SONET) elements. But, owing to the relatively slow response time of these devices, of the order of hundreds of milliseconds to tens of seconds, these networks are limited to fast circuit switching applications, at best. In order to take full advantage of the possibilities afforded by wavelength division multiplexed (WDM) data links, new kinds of network elements with vastly improved performance are required. In particular, the use of WDM strategy requires optical filters for adding and dropping single wavelength channels in certain network nodes.

The emerging technology of photonic crystals (PhCs) [1] can be suitably exploited to design and make optical devices for WDM applications. The novel and unique way to control many features of electromagnetic radiation offers the opportunity of developing photonic band gap (PBG) structures such as waveguides, splitters, resonant cavities, and so on [2]. Since the first application of photonic crystal based WDM structures by Fan, *et al*. [3], several researchers proposed and experimentally demonstrated optical trapping and dropping functions by exploiting resonant tunneling [4], superprism [5], cavity-waveguiding coupling [6] phenomena in one-dimensional (1D) [7], two-dimensional [8,9,10] and three-dimensional PhCs [11].

Another typical configuration of photonic band gap filters incorporates Bragg gratings. As it is well known, Bragg-grating filters are an attractive choice when the requirements for intra-channel crosstalk are stringent. But the spectral response of uniform Bragg gratings suffers from large side lobes, which deteriorate the inter-channel crosstalk or cause poor bandwidth utilization. In practice, often, non uniform tapered apodized or chirped gratings, are used to exploit their special signal processing characteristics [12, 13, 14]. Moreover, conventional Bragg-grating filters, suitable for WDM application, require a high number of periods. The PBG Bragg-grating filters are composite structures which consist, in general, of a short length grating with a photonic band gap structure. As an example, in [15] a finite length grating assisted coupler was integrated with a linear multilayer PBG mirror, while in [16] a DWDM demultiplexer consisting of rectangular shaped frequency filters connected in series was proposed, the rectangular pass band filters being formed with an apodized 1D PhC structure on a ridged semiconductor waveguide.

In this paper we propose a multiplexing-demultiplexing (MUX-DEMUX) structure based on an index-confined photonic band gap waveguide: the dropping of electromagnetic waves having a given frequency or a certain frequency band is obtained via a nonuniform grating where the otherwise uniform period sequence is broken by a "defect layer" having an opportune length along the propagation direction. The structure can be regarded like a phase-shifted grating [17,18]. Standard phase shifted Bragg filters consists of M uniform grating sections with length L_1, L_2, …..L_M , and (M-1) intermediate regions, providing the phase shifts ϕ_1, ϕ_2,…… ϕ_M, all stacked in series. These filters exhibit nearly rectangular pass band characteristics, *i.e.,* a drastic slope to the stop band. The finite width of the stop band in the center of which the transmission takes place and the bandwidth needed for sensitivity penalty-free transmission are serious drawbacks in terms of channel number and channel selection for the use of these phase-shifted filters in WDM systems. To overcome these limits, more complicated structures have to be considered. For adjusting the pass band central wavelength in each filter to the corresponding channel waveguide, grating regions with different periods have to be included. To increase the channel number, the ratio between the stop band width

#1976 - $15.00 US Received December 19, 2002; Revised February 03, 2003

and the transmission bandwidth ought to be high: therefore gratings characterized by a maximum coupling factor κ are necessary, the width of the stop band being proportional to κ. The structure proposed in this paper, having a single defect layer, appears to be even simpler and shorter than the compound phase-shifted Bragg grating reported in [17]. The capability of the proposed structure to shape and broaden the pass-band that arises in the middle of the grating stop band and, then, the channel number which can be settled in the stop band are strongly dependent on the defect layer parameters. Here, using a bidirectional beam propagation method based on the method of lines (MoL-BBPM) [19], we report the design criteria of multichannel wavelength demultiplexers characterized by suitable values of the pass band and the stop band, as a function of the defect position and length. Finally, we present an eight-channel MUX-DEMUX operating in the second transmission window of the optical fiber telecommunication systems characterized by a channel spacing useful for WDM systems and drastically reduced device sizes compared with those of a conventional Bragg grating [20].

2. Theoretical remarks

The MoL-BBPM algorithm is based on two operators and works in two steps [19]. The first operator describes the one-way propagation (positive longitudinal +z direction), while the latter determines the reflection from a generic discontinuity along the structure longitudinal direction. In the first step, the two operators are used in the forward propagation to calculate the transmitted and the reflected fields at each discontinuity along the structure by imposing the continuity of the electromagnetic (EM) field tangential components at the discontinuity interfaces. Successively, in the second step, the backward negative longitudinal -z direction propagation is accounted and the new transmitted and reflected fields are evaluated, taking into account the reflection contribution calculated in the previous step. Then, all the forward and the backward waves, so calculated at each computational longitudinal section, are added up. This procedure is iteratively applied till to reach the desired convergence. The convergence criterion is based on the comparison between the fields at the output section (z=L) calculated in two successive iterations.

In each discontinuity section along the longitudinal z axis, the MoL-BBPM code assumes, for the wave equation along each line, the following expression for the vector $\boldsymbol{\varphi}$, the components of which are the scalar potentials φ_i in the original domain:

$$\frac{d^2\boldsymbol{\varphi}}{du^2} - \mathbf{Q}\boldsymbol{\varphi} = 0 \tag{1}$$

In Eq. (1) $\mathbf{Q}$ is the matrix of the discretized difference operator and $u=k_0 z$ is the normalized longitudinal axis, k_0 being the vacuum wavenumber. Because the matrix $\mathbf{Q}$ is not diagonal, the potentials φ_i are each other coupled and the wave Eq. (1) cannot be solved in this form. By diagonalizing $\mathbf{Q}$, both the vector of the eigenvalues λ and the matrix of the eigenvectors are evaluated:

$$\frac{d^2\overline{\boldsymbol{\varphi}}}{du^2} - \lambda^2\overline{\boldsymbol{\varphi}} = 0 \tag{2}$$

Equation (2) is analytically solved:

$$\overline{\boldsymbol{\varphi}}(u) = \mathbf{F}\, e^{-\lambda u} + \mathbf{B}\, e^{\lambda u} \tag{3}$$

where $\mathbf{F}\, e^{-\lambda u}$ and $\mathbf{B}\, e^{\lambda u}$ are the contributions of the forward and the backward fields in the transformed domain, respectively. The field $\boldsymbol{\varphi}(u)$ in the original domain can be obtained by

#1976 - $15.00 US Received December 19, 2002; Revised February 03, 2003

the inverse domain transformation. In order to obtain the reflection operator, Eq. (2) is analytically solved for the forward and backward travelling waves in both the left (L) and the right (R) regions of each discontinuity. After having calculated the forward coefficient F_L of Eq. (3) in the left region, the unknown left backward and right forward coefficients B_L, F_R are evaluated by placing the right backward coefficient B_R=0 and by matching the electromagnetic field transverse components at the discontinuity interfaces.

A preliminary accuracy analysis of the MoL-BBPM applied to an index-confined 1D-PBG waveguide, *i.e.*, a periodically strong etched waveguide grating, originating from the European COST 268 action, has given excellent results compared with those obtained by two home-made simulators based on the analytical Transfer Matrix Method (TMM) and the numerical 2D Finite Difference Time Domain (FDTD) method [19]. On the other hand, the CPU computing times (of about 5 min on a personal computer Pentium III 800 MHz) of the MoL-BBPM are only a little longer than those occurring for the TMM, while are much more shorter than those evaluated by the FDTD (of about 180 min).

3. Numerical results

First we consider a simple finite-length standard IC-1D-PBG waveguide, *i.e,*. a single mode optical slab waveguide equipped with an appropriate periodically corrugated overlay (see Fig. 1 without the defect waveguide). The GaAs/Al_2O_3 waveguide is characterized by the following parameters: core refractive index n_g = 3.4, substrate refractive index n_s = 1.6 at the operating wavelength λ = 1300 nm; core thickness d_g = 240 nm. The grating is constituted by a finite number of N alternating layers of air (n_a = 1) and GaAs having the same width (w_1 = w_2 = 116 nm), spatial period Λ = w_1 + w_2 = 232 nm and tooth depth h = 60 nm.

According to the results shown in [19], we have verified that also for the geometrical and the physical data of the examined structure, the transmission characteristics depend on the number of spatial periods N_Λ, the tooth depth h and by the duty cycle, *i.e.*, the ratio of tooth width to groove width w_2/w_1. In particular we have found that, for N = 63 alternating layers and number of spatial periods N_Λ = 32, the structure acts as a stop band reflection filter, for the TE polarization, centered at the Bragg wavelength λ_B = 1305 nm, with a 3 dB bandwidth equal to 50 nm (see blue line in Fig. 2). For the chosen geometrical and physical parameter values, the Bragg wavelength of the waveguide grating having rectangular grooves can be evaluated according to the approximated formula obtained by neglecting the scattering into radiation modes:

$$\lambda_B \cong 2(n_t w_2 + n_g w_1) \qquad (4)$$

where n_t and n_g are the refractive effective indices of the two three-layered waveguides corresponding to the tooth and to the groove of the Bragg grating unit cell, respectively.

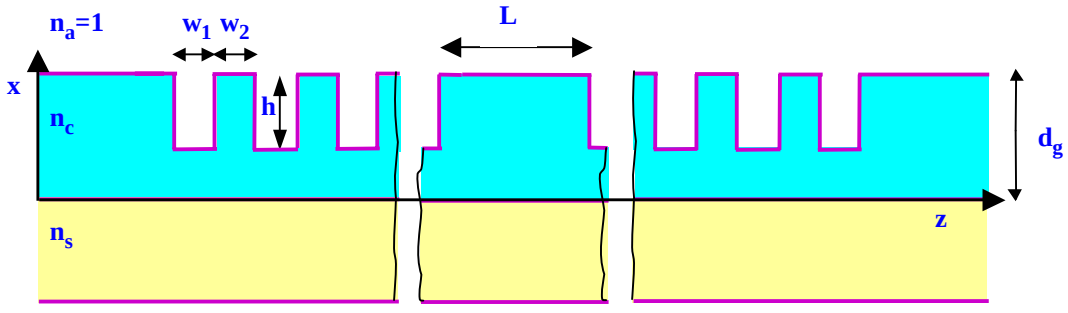

Fig. 1. Layout of the IC-1D-PBG filter.

#1976 - $15.00 US
Received December 19, 2002; Revised February 03, 2003

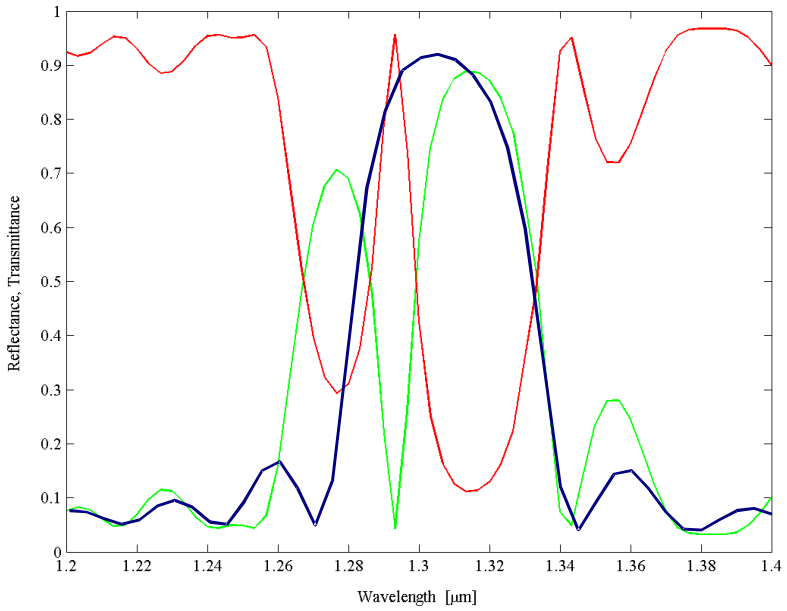

Fig. 2. Reflectance (green line) and transmittance (red line) spectra for defect waveguide length L = 1.97 μm. Reflectance (blue line) for the N = 32 period waveguide without defect.

By calculation, for the TE polarization we find $n_t = 2.937$ for the waveguide having thickness d_g and $n_g = 2.738$ for the waveguide having thickness (d_g-h), thus Eq. (4) gives $\lambda_B = 1316$ nm. However, the "exact" Bragg wavelength value directly obtained by the MoL-BBPM is $\lambda_B = 1305$ nm**.**

The incorporation of defect regions gives rise to narrow band transmission windows inside the stop band of the finite-length standard Bragg grating. The considered defect in this analysis is the substitution of a "groove" with a "tooth", *i.e.*, with a segment of GaAs/Al_2O_3 waveguide, having core thickness d_g. Really the introduction of a single defect in any part of the grating does not give rise to significant changes in the stop band while the increase of the defect number, introduced especially in the central part of the grating, gives the maximum efficiency in terms of maximum reflectance in the stop band and channel bandwidth reduction. In fact, the transmittance and reflectance spectra of the structure do not change significantly when the defects are all confined in the neighbourhood of either the input or the output ports, because in this case the defect inclusion induces only the optical shift of the propagating signal in the input or the output port, respectively. On the other hand, the signal optical shift in both the longitudinal propagation directions, induced on the propagating signal along the defect region, assumes an increasing important role as the waveguide inclusion is shifted from the extreme to the central position of the Bragg grating. Anyway, a further increase of the defect number, to parity of device length, reducing drastically the total spatial period number, deteriorates the filter spectral response. For this reason, the spatial period number has been fixed to 32 and a unique defected region L long is introduced in the middle of the IC-1D-PBG waveguide.

Figure 1 shows the layout of the proposed IC-1D-PBG filter: it consists of two equal PBG grating waveguides which include the defect region. The defect region consists of a segment of GaAs/Al_2O_3 waveguide having length L and core depth d_g.

#1976 - $15.00 US
Received December 19, 2002; Revised February 03, 2003

The performance of the IC-1D-PBG waveguide to act as WDM filter is strongly influenced by the defect waveguide length L. As an example, by fixing the defect waveguide length L = 1.97 μm and considering a total number of alternating grating layers N = 63, the transmission spectrum, depicted in Fig. 2, exhibits in the wavelength range 1260-1350 nm two stop bands separated by a transmission channel having central wavelength λ_c = 1293 nm, 3 dB bandwidth B_λ = 12 nm, maximum value of transmission coefficient T = 0.95 and minimum reflection coefficient R = 0.05. The stop bands centered at λ = 1275 nm and λ = 1318 nm exhibit a maximum R value of 0.70 and 0.90, respectively. By increasing L to 3.6 μm the spectra do not change significantly, the only difference being the value of the reflectance in the first stop band which reaches the maximum of 0.90.

The channel number N_c increases by increasing the defect waveguide L length. This parameter becomes fundamental to design a demultiplexer: the empirical relationship between the channel number, the defect waveguide L length and the Bragg wavelength λ_B derived by simulations is $N_c \cong L / 2\lambda_B$. In the case of L = 35 μm, we calculate N_c =12 channels which increase to 22 for L= 67 μm. Anyway, in the following investigations we will count the number of channels by considering transmission channels only those having, on their left and right, stop bands characterized by reflection coefficient values greater than 0.75. This number will be named useful channel number $N_{c,u}$. Figure 3 shows the useful channel number against the defect waveguide L length. Following the definition, we count $N_{c,u}$ = 8 channels for L = 35 μm: this number increases to 18 for L= 67 μm.

Figure 4 shows the transmission and reflection spectra in the case of defect waveguide length L = 35 μm. As we can infer from the depicted spectra, the system of transmission channels and stop bands is always in the same wavelength range 1260-1350 nm: therefore, if the channel number increases, the channel bandwidth and the channel spacing almost proportionally decrease. Table 1 illustrates the characteristic parameters (useful channel number, the channel spacing Δ and the 3 dB bandwidth) of the index confined

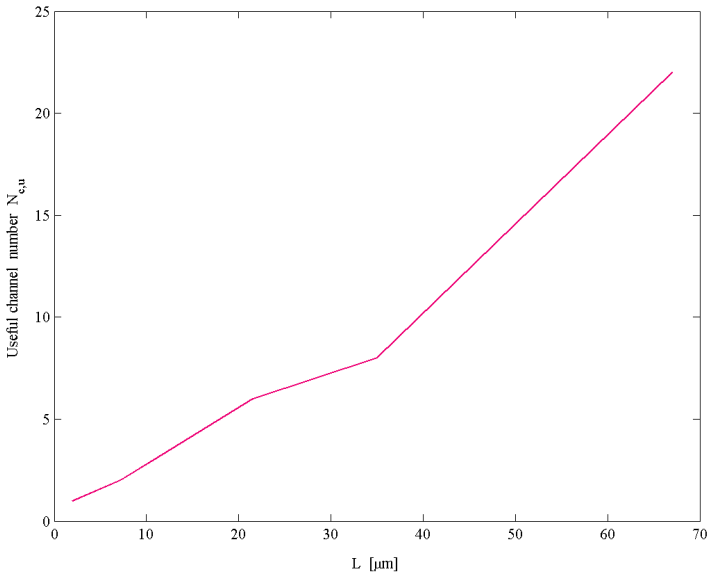

Fig. 3. Useful channel number $N_{c,u}$ as a function of the defect waveguide L length.

#1976 - $15.00 US
Received December 19, 2002; Revised February 03, 2003

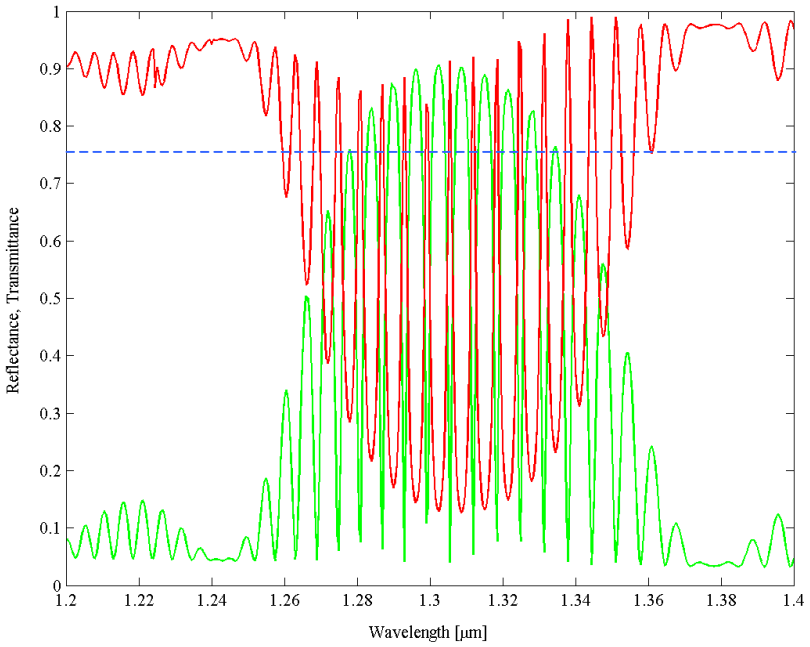

Fig. 4. Reflectance (green line) and transmittance (red line) spectra for defect waveguide length L = 35 μm. $N_{c,u}$ = 8 useful channels are evident in the wavelength range from 1.26 μm to 1.36 μm.

Table 1. Characteristic parameters of the index confined photonic band gap demultiplexer as a function of the defect waveguide L length.

Defect waveguide L length [μm]	Useful channel number	Channel spacing Δ [nm]	3 dB bandwidth B_λ [nm]
7.2	**2**	**26**	**6**
10.8	**3**	**12**	**4**
21.6	**6**	**7.5**	**2.5**
35	**8**	**6**	**2**
37	**9**	**4.8**	**1.8**
67	**18**	**2.5**	**0.8**

photonic band gap demultiplexer as a function of the defect waveguide L length. As we can see from Fig. 4, the index confined photonic band gap demultiplexer characterized by a defect waveguide length L = 35 μm exhibits a 3 dB bandwidth for each channel of about B_λ = 2 nm, while the channel spacing is 6 nm. These values drastically reduce when an index confined photonic band gap demultiplexer characterized by a defect waveguide length of L = 67 μm is considered: in this case a 3 dB bandwidth of only 0.8 nm and a channel spacing of 2.5 nm are obtained. The spectral behaviour of the examined structures can be understood by considering a Fabry-Perot cavity of length L having distributed reflectors at each end

#1976 - $15.00 US Received December 19, 2002; Revised February 03, 2003

consisting of short strong Bragg gratings. This is a special case of filter with one-phase shift section [17,18]. In this sense, the reflection and the transmission spectra can be calculated in terms of transfer matrices of each section constituting the phase-shift Bragg grating. Therefore, the spectral behaviour is linked to the cavity length, the refractive index of the cavity and the Bragg wavelength. The empirical approximated formula of the channel number N_c, obtained by the MoL-BBPM simulations, accounts for these terms.

Moreover, we can observe in Tab.I that the ratio channel spacing/channel 3 dB bandwidth remains practically constant and equal to about 3 by changing the defect length L from 10.8 μm to 67 μm, thus assuring constant optical crosstalk between adjacent channels. In particular, by following the approximate expression of the optical channel crosstalk, evaluated in the case of transmission spectrum of each channel described by a Gaussian distribution [21], given by: $CT \cong -6.02\ (\Delta/B_\lambda)^2$, resulting for our structure $\Delta/B_\lambda \cong 3$, we have obtained $CT \cong -54$ dB.

In order to put in evidence the confining performance of the proposed demultiplexer waveguide, Figs. 5 and 6 show the EM field evolution of the electric field E_y component calculated by the MoL-BBPM, for the wavelength values of maximum transmission (λ = 1299 nm, R = 0.10, T = 0.90) and of 3 dB bandwidth (λ = 1300 nm, R = 0.45, T = 0.55), respectively. The pink lines draft the geometrical profile of the IC-1D-PBG filter with the inclusion of the defect waveguide as in Fig. 1. The different behaviour of the EM field propagation for the two wavelength values is outlined in Figs. 7 and 8, that sketch the patterns of the electric field E_y component of the signal launched in the input port (blue line), the reflected field in the input port (red line) and the transmitted field in the output port (green line). We can see that for the wavelength of maximum transmission (λ = 1299 nm) the reflected field E_y component (R = 0.10) is negligible with respect to the transmitted one, whereas for the 3 dB bandwidth wavelength (λ = 1300 nm) the two reflected and transmitted components assumes almost the same values (R = 0.45, T = 0.55).

Finally, preliminary results, obtained by applying the MoL-BBPM to a similar structure of Fig. 1 made of SiO_2 substrate (n_s = 1.45), Si_3N_4 core (n_c = 2), $w_1 = w_2$ = 215 nm, N = 39, d_g = 500 nm, h = 250 nm, have evidenced excellent properties to be exploited for the design of WDM filters useful for applications in the third window of the optic fiber telecommunications at the central wavelength λ = 1485 nm.

4. Conclusion

The filtering properties of an index-confined finite photonic band gap waveguide, incorporating a phase-shifted grating have been investigated. The capability of dropping the EM waves having specific frequencies has been shown to depend quite sensitively upon the defect region length. This PBG structure is very suitable for WDM applications.

#1976 - $15.00 US Received December 19, 2002; Revised February 03, 2003

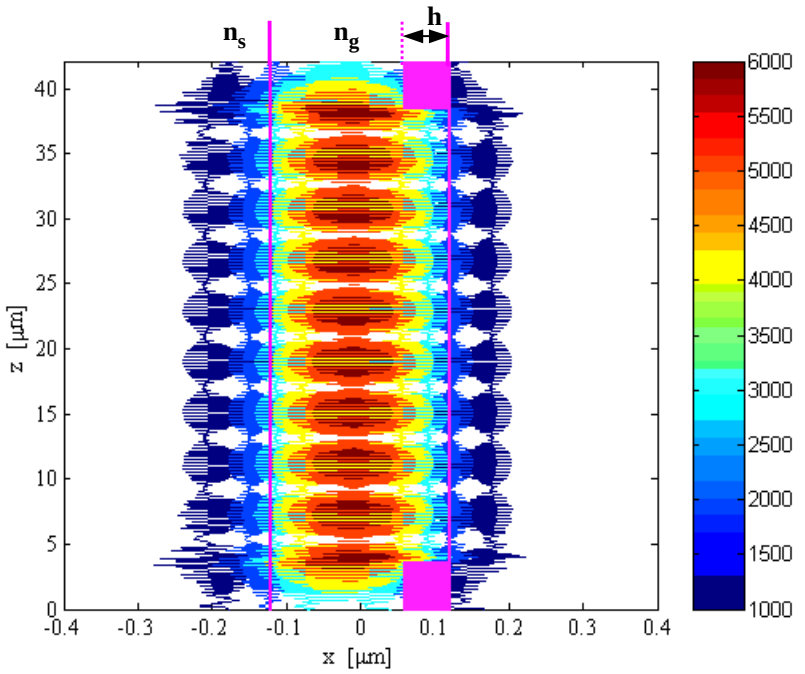

Fig. 5. Contour lines of the three-dimensional evolution of the electric field E_y (color scale in V/m) component for defect waveguide length L = 35 μm: λ = 1299 nm and R = 0.10, T = 0.90.

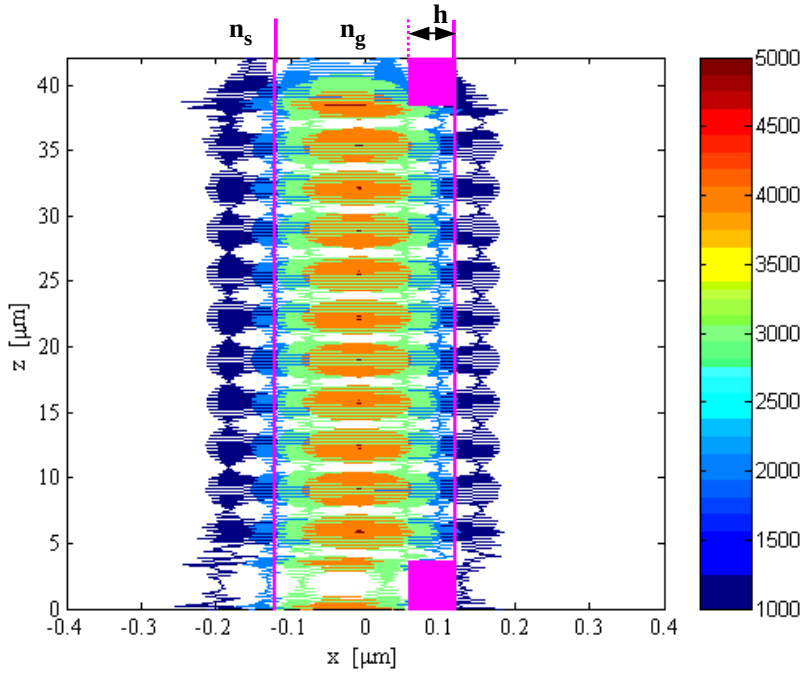

Fig. 6. Contour lines of the three-dimensional evolution of the electric field E_y (color scale in V/m) component for defect waveguide length L = 35 μm: λ = 1300 nm and R = 0.55, T = 0.45.

#1976 - $15.00 US
Received December 19, 2002; Revised February 03, 2003

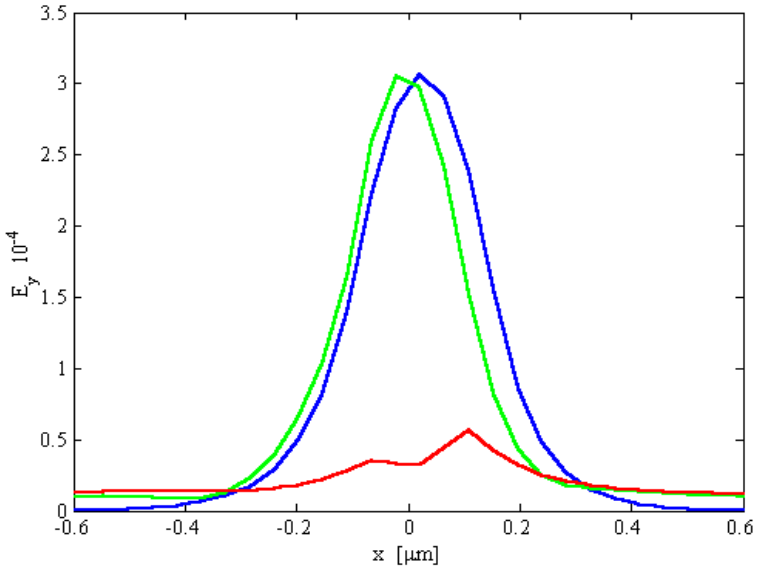

Fig. 7. Patterns of the input (blue line), reflected (red line) and transmitted (green line) electric field E_y component for λ = 1299 nm and R = 0.10, T = 0.90.

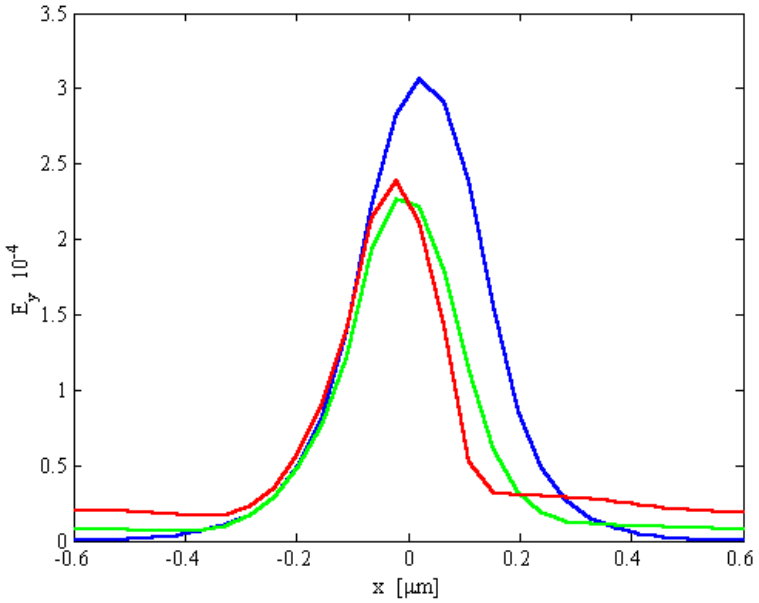

Fig. 8. Patterns of the input (blue line), reflected (red line) and transmitted (green line) electric field E_y component for λ = 1300 nm and R = 0.55, T = 0.45.

#1976 - $15.00 US
Received December 19, 2002; Revised February 03, 2003